Biological soil crusts accelerate the nitrogen cycle through large NO and HONO emissions in drylands

Bettina Weber[a,1], Dianming Wu[a,b,c], Alexandra Tamm[a], Nina Ruckteschler[a], Emilio Rodríguez-Caballero[a], Jörg Steinkamp[d], Hannah Meusel[a], Wolfgang Elbert[a,b], Thomas Behrendt[e], Matthias Sörgel[b], Yafang Cheng[a], Paul J. Crutzen[f], Hang Su[a], and Ulrich Pöschl[a]

[a]Multiphase Chemistry Department, Max Planck Institute for Chemistry, 55128 Mainz, Germany; [b]Biogeochemistry Department, Max Planck Institute for Chemistry, 55128 Mainz, Germany; [c]Key Laboratory of Agricultural Water Research, Center for Agricultural Resources Research, Institute of Genetic and Developmental Biology, Chinese Academy of Sciences, Shijiazhuang 050021, China; [d]Senckenberg Biodiversity and Climate Research Centre, 60325 Frankfurt am Main, Germany; [e]Biogeochemical Processes Department, Max Planck Institute for Biogeochemistry, 07745 Jena, Germany; and [f]Air Chemistry Department, Max Planck Institute for Chemistry, 55128 Mainz, Germany

Edited by Steven C. Wofsy, Harvard University, Cambridge, MA, and approved October 23, 2015 (received for review August 10, 2015)

Reactive nitrogen species have a strong influence on atmospheric chemistry and climate, tightly coupling the Earth's nitrogen cycle with microbial activity in the biosphere. Their sources, however, are not well constrained, especially in dryland regions accounting for a major fraction of the global land surface. Here, we show that biological soil crusts (biocrusts) are emitters of nitric oxide (NO) and nitrous acid (HONO). Largest fluxes are obtained by dark cyanobacteria-dominated biocrusts, being ∼20 times higher than those of neighboring uncrusted soils. Based on laboratory, field, and satellite measurement data, we obtain a best estimate of ∼1.7 Tg per year for the global emission of reactive nitrogen from biocrusts (1.1 Tg a^{-1} of NO-N and 0.6 Tg a^{-1} of HONO-N), corresponding to ∼20% of global nitrogen oxide emissions from soils under natural vegetation. On continental scales, emissions are highest in Africa and South America and lowest in Europe. Our results suggest that dryland emissions of reactive nitrogen are largely driven by biocrusts rather than the underlying soil. They help to explain enigmatic discrepancies between measurement and modeling approaches of global reactive nitrogen emissions. As the emissions of biocrusts strongly depend on precipitation events, climate change affecting the distribution and frequency of precipitation may have a strong impact on terrestrial emissions of reactive nitrogen and related climate feedback effects. Because biocrusts also account for a large fraction of global terrestrial biological nitrogen fixation, their impacts should be further quantified and included in regional and global models of air chemistry, biogeochemistry, and climate.

biological soil crusts | nitric oxide | nitrous acid | nitrogen | trace gas emission

Nitrogen oxides and nitrous acid are key species in the global cycling of nitrogen and in the production of ozone and hydroxyl radicals, regulating the oxidizing power and self-cleaning capacity of the atmosphere (1–3). Nitric oxide (NO) emissions from soil have long been known (4–6), and recent studies found that also nitrous acid (HONO) can be released from biogenic soil sources (7, 8). Reactive nitrogen emissions from soil bacteria are usually stimulated by nitrogen input from chemical and manure fertilizer or atmospheric deposition (7–9). In dryland regions, where nitrogen fertilization and deposition tend to be low (10), enhanced concentrations of NO have been observed after rain and attributed to ground sources (9, 11), but measured soil emissions were too small to explain the atmospheric observations (8, 12).

Biological soil crusts (biocrusts) occurring on ground surfaces in drylands throughout the world consist of cyanobacteria, lichens, mosses, and algae plus heterotrophic bacteria, fungi, and archaea in varying proportions. Depending on the dominating photoautotrophic component, they are classified into the major groups of cyanobacteria-, lichen-, and moss-dominated biocrusts (13). Fossil records suggest that biological crusts similar to today's cyanobacterial biocrusts formed the earliest terrestrial ecosystems in Earth's history over 3 billion years ago (14, 15). Today, they are still pioneers in the colonization and succession of bare grounds such as burnt areas, loose sand, and volcanic deposits (16, 17). In a recent study, Elbert et al. (18) found that biocrusts, i.e., cryptogamic ground covers in desert and steppe ecosystems, are fixing large amounts of atmospheric nitrogen, with a best estimate of ∼26 Tg a^{-1}, corresponding to ∼40% of the most recent Intergovernmental Panel on Climate Change (IPCC) estimate for global terrestrial biological nitrogen fixation (19). But what are the consequences of nitrogen fixation by biocrusts? Incubation studies have shown that biocrusts can release nitrogen oxides (20–22), while field and model studies suggested large emissions of nitrogen oxides from drylands, raising questions about their origin (9, 11, 23, 24).

In this study, we investigate the emission of reactive nitrogen from biocrusts in drylands on continental and global scales. For this purpose, we measured NO and HONO fluxes from the main types of biocrusts using a controlled dynamic chamber method. Earlier studies have shown that emissions obtained by this technique are consistent with field measurements (25, 26). Samples of bare soil without biocrust cover collected at the same locations

Significance

Biological soil crusts (biocrusts), occurring on ground surfaces in drylands throughout the world, are among the oldest life forms consisting of cyanobacteria, lichens, mosses, and algae plus heterotrophic organisms in varying proportions. They prevent soil erosion and nurture ecosystems by fixing carbon and nitrogen from the atmosphere. Here, we show that the fixed nitrogen is processed within the biocrusts, and during this metabolic activity, nitrogen oxide and nitrous acid are released to the atmosphere. Both of these gases are highly relevant, as they influence the radical formation and oxidizing capacity of the lower atmosphere, also interacting with climate change. In drylands, biocrusts appear to play a key role both in nitrogen fixation and the release of atmospheric reactive nitrogen.

Author contributions: B.W., W.E., T.B., P.J.C., and U.P. designed research; B.W. and A.T. collected samples; D.W., A.T., and N.R. conducted trace gas measurements; E.R.-C. and J.S. did global upscaling and created maps; H.M. and M.S. contributed new reagents/analytic tools; B.W., D.W., A.T., N.R., E.R.-C., J.S., Y.C., H.S., and U.P. analyzed data; and B.W. and U.P. wrote the paper.

The authors declare no conflict of interest.

This article is a PNAS Direct Submission.

Freely available online through the PNAS open access option.

[1]To whom correspondence should be addressed. Email: b.weber@mpic.de.

This article contains supporting information online at www.pnas.org/lookup/suppl/doi:10.1073/pnas.1515818112/-/DCSupplemental.

were analyzed for comparison. Emissions during full wetting–drying cycles were combined with biocrust composition and global distribution data as well as satellite-retrieved precipitation information to obtain best estimates of global annual NO and HONO release.

Results and Discussion

All types of biocrusts showed characteristic patterns of NO and HONO emission fluxes as a function of soil water content (SWC) (Fig. 1). Cyanobacteria-dominated crusts exhibited a sharp peak around 20–25% water-holding capacity (WHC) (i.e., the maximum amount of water absorbed by a soil), indicating that NO and HONO are formed during nitrification by bacteria or archaea under aerobic conditions (6, 8, 27). In contrast, the emissions of chlorolichen- and moss-dominated crusts extended over a wider range of SWC (~20–80% WHC), suggesting that both nitrification and denitrification under aerobic and anaerobic conditions may be involved (28).

In Fig. 2*A*, the average maximum emission fluxes at optimum soil moisture conditions are shown for all sample types investigated. The highest average values were recorded for dark cyanobacteria-dominated biocrusts: 208 ± 15 ng·m^{-2}·s^{-1} of nitrogen in NO (NO-N) and 173 ± 18 ng·m^{-2}·s^{-1} of nitrogen in HONO (HONO-N) (best estimate ± SE) (*SI Appendix*, Table S1). In contrast, the average maximum emission fluxes of bare soil samples were lower by more than a factor of 20 (9 ± 3 ng·m^{-2}·s^{-1} for NO-N and 5 ± 2 ng·m^{-2}·s^{-1} for HONO-N). For soil samples collected from a wide range of ecosystems around the world, Oswald et al. (8) had determined emission fluxes from <1 to ~50 ng·m^{-2}·s^{-1} for NO-N and ~30 ng·m^{-2}·s^{-1} for HONO-N, whereas only two strongly fertilized soils exhibited emission fluxes around ~200 ng·m^{-2}·s^{-1}. In former biocrust studies, NO emissions were determined to be minor by means of chamber experiments (29),

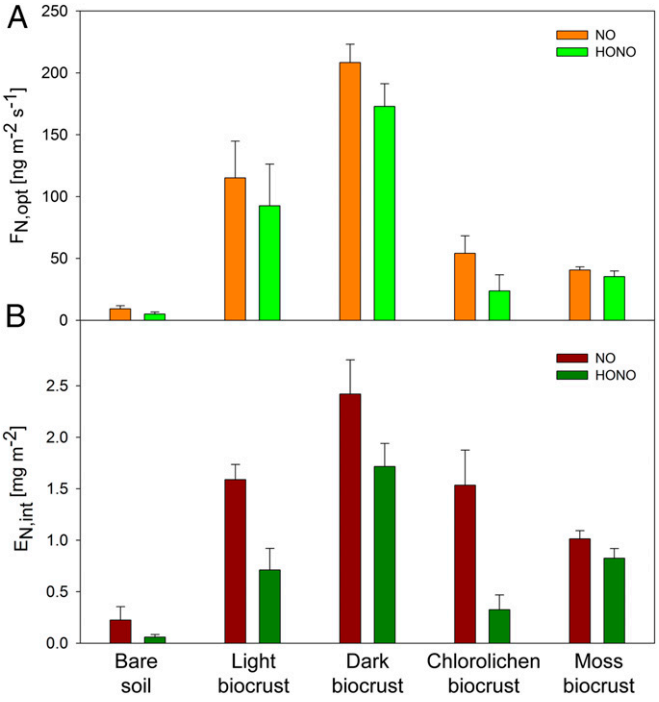

Fig. 2. Emissions of NO-N and HONO-N from different types of biocrusts and bare soil. (*A*) Average maximum emission fluxes with SE of means under optimum water conditions. (*B*) Average emissions during a full wetting and drying cycle with SE of means. Emission fluxes were measured at 25 °C and in the dark to avoid photolytic reactions. All biocrust types and bare soil were measured in replicates (n = 4).

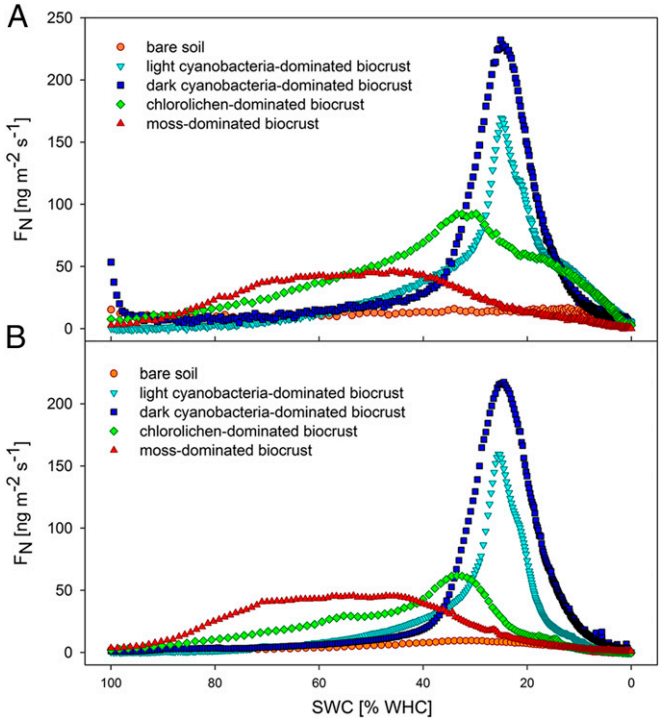

Fig. 1. Characteristic emission patterns of NO-N and HONO-N from different types of biocrusts and bare soil at varying soil water contents. (*A*) NO-N emissions. (*B*) HONO-N emissions. For better visibility of the symbols, only every 2nd (light cyanobacteria-dominated), 5th (dark cyanobacteria-dominated), or 10th (chlorolichen-dominated, moss-dominated biocrusts, bare soil) value is shown.

whereas in continuous flux measurements, McCalley and Sparks (24) determined emissions of up to 60 ng·m^{-2}·s^{-1} of NO-N on Mojave Desert soils with ~20% biocrust coverage. Due to the high soil temperatures, the latter assumed these emissions to be abiotic, whereas our experiments revealed that, after sterilization, almost no NO and HONO emissions were measured on previously emitting samples (Fig. 3).

The total emissions of NO-N and HONO-N integrated over a full wetting and drying cycle are shown in Fig. 2*B*. Again, the highest values were obtained for dark cyanobacteria-dominated biocrusts (2.4 ± 0.3 mg·m^{-2} NO-N and 1.7 ± 0.2 mg·m^{-2} of HONO-N), whereas the integrated emissions of bare soil were more than an order of magnitude lower (*SI Appendix*, Table S2).

Combining our chamber measurements with related field and literature data on biocrust composition, we investigated the atmospheric relevance of reactive nitrogen emissions from biocrusts in steppe and desert ecosystems on continental and global scales. Following the approach of Elbert et al. (18), we calculated best estimates and uncertainty ranges for the emissions of reactive nitrogen from biocrusts in the course of a precipitation event (wetting and drying cycle), for which we obtained ~0.7 ± 0.1 mg·m^{-2} of NO-N and ~0.4 ± 0.1 mg·m^{-2} of HONO-N as detailed in *SI Appendix* (*SI Appendix*, Tables S2–S4).

By multiplication with satellite-retrieved annual precipitation data, we obtained an estimate for the global distribution of reactive nitrogen emissions from biocrusts in drylands, i.e., hot deserts and steppe, as shown in Fig. 4. On continental scales, the sum of reactive nitrogen emissions is highest in Africa (~0.7 ± 0.1 Tg a^{-1}), South America (~0.4 ± 0.1 Tg a^{-1}), and Asia (~0.2 ± 0.03 Tg a^{-1} of NO-N and HONO-N) and lowest in Europe (*SI Appendix*, Fig. S2 and Table S5). Globally integrated, the emissions amount to ~1.1 ± 0.1 Tg a^{-1} of

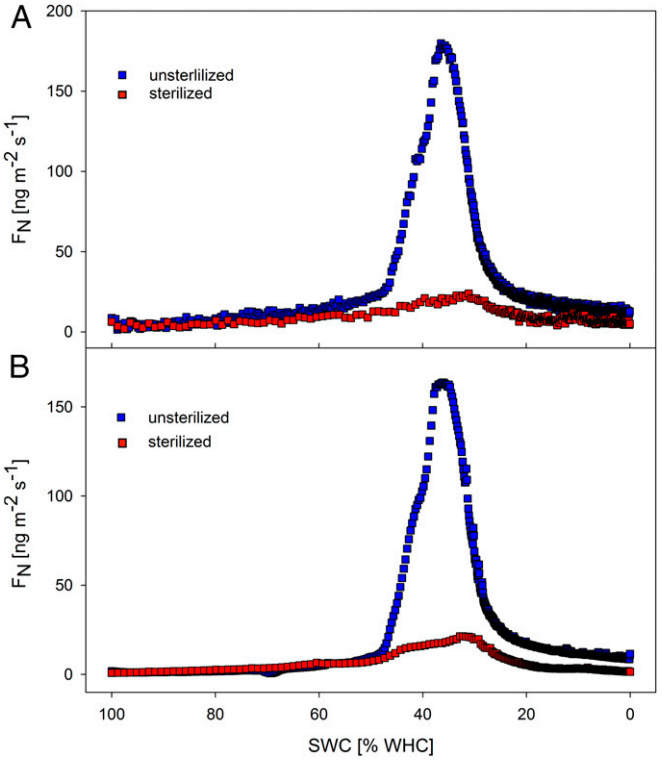

Fig. 3. NO and HONO emissions of dark cyanobacteria-dominated biocrust before and after sterilization. (*A*) NO-N emissions. (*B*) HONO-N emissions. For better visibility of the symbols, only every 3rd (unsterilized sample) and 10th (sterilized sample) value is shown.

NO-N and ~0.6 ± 0.1 Tg a^{-1} of HONO-N, summing up to ~1.7 ± 0.3 Tg a^{-1} of reactive nitrogen emissions.

Process-based bottom-up models, as the widely used algorithms of Yienger and Levy (30) and GEOS-CHEM (31), predicted global NO-N emissions of 5.5 and 5.3 Tg a^{-1} from soils, respectively, whereas data-based top-down approaches identified substantially larger fluxes [8.9 Tg a^{-1} (23); 8.4 Tg a^{-1} (9)] with major sources being located in dryland regions (9, 11, 23). Our results indicate that these dryland emissions are largely driven by biocrusts rather than the underlying soil, and may explain a major fraction of the discrepancy between bottom-up and top-down modeling approaches.

Fig. 5 illustrates the relevance and approximate magnitude of biocrust nitrogen fluxes as part of the overall biological terrestrial nitrogen fluxes. Their uptake of molecular nitrogen corresponds to as much as ~40% of current estimates of terrestrial biological nitrogen fixation. The biocrust emissions of reactive nitrogen (HONO-N plus NO-N) correspond to ~20% of current estimates of reactive nitrogen emissions from soils under natural vegetation [7.3 Tg a^{-1} (19)] or, for reference, approximately one-half the amount of reactive nitrogen annually released by agriculture [3.7 Tg a^{-1} (19)]. Thus, despite the fact that biocrusts only grow within the uppermost few millimeters of dryland soils, they largely influence biological N fixation and reactive trace gas emissions on a global scale. The fraction of fixed N released by soil ranges between 5% and 16%, and that by biocrusts between 3% and 14%, thus covering an almost identical range, which may indicate similar processes in both cycles.

Recent investigations of cyanobacteria, lichens, and mosses suggest that biocrusts can also emit substantial amounts of N_2O (32). Further investigations comprising multiple nitrogen compounds and isotopes should unravel the interplay of different chemical and biological species and processes in the cycling of nitrogen by biocrusts (33–36).

In the course of global change, the relevance of nitrogen cycling by biocrusts may increase with an expansion of dryland ecosystems currently covering around ~40% of the global land surface (37). On the other hand, biocrusts are threatened by land use change, and changing precipitation patterns (38) may affect their composition, distribution, and physiological activity. The interactions and effects of biocrusts constitute a complex and potentially strong feedback loop in the history and evolution of the Earth system. Thus, the influence of biocrusts on the nitrogen cycle should be further quantified and included in regional and global models of air chemistry, biogeochemistry, and climate.

Methods

Biocrust Sampling. Biocrust samples were collected in the vicinity of BIOTA observatory 22 (Soebatsfontein; 30.1865°S, 17.5433°E) about 60 km south of Springbok in the Succulent Karoo, South Africa. Samples from this region turned out to be characteristic for warm deserts around the globe (18, 39, 40). In October 2013 and 2014, spatially independent replicate samples were collected of each of the four biocrust types: (*i*) initial cyanobacteria-dominated biocrusts (light biocrust), (*ii*) dark cyanobacteria-dominated biocrusts with cyanolichens (dark biocrust), (*iii*) chlorolichen-dominated biocrusts with *Psora decipiens* as dominating lichen species (chlorolichen biocrust), and (*iv*) moss-dominated biocrusts with *Ceratodon purpureus* as dominating moss species (moss biocrust), and of bare uncrusted soil. For an in-depth description of the different types of biocrusts, see Dojani et al. (13, 16). The samples were collected by means of stainless-steel cylinders (5.0-cm diameter, 2.6 cm high), were then air-dried in the camp to minimize metabolic activity, and transported to the Max Planck Institute for Chemistry in Mainz for analyses. There they were stored in the refrigerator at 5 °C until measurements.

Measurement of Samples. Samples were watered and then placed into a Teflon chamber to analyze trace gas fluxes during the drying process. The chamber was purged with purified dry air, and thorough mixing of the chamber headspace was achieved by a fan. Release and mixing ratios of HONO, NO, NO_2, and H_2O in the chamber were measured at the chamber outlet. The chamber was kept at 25 °C, and measurements were conducted in the dark to avoid photolytic reactions. NO and NO_2 were measured with a gas chemiluminescence detector and HONO with a long path absorption photometer. The loss in soil water content during the experiment was determined by initial weighing and measurement of temperature and relative humidity at the chamber outlet. After complete drying, the sample was removed from the chamber and placed in a drying oven to determine the exact dry weight of the sample.

Maximum emission rates, duration of emission events, and correlations between NO and HONO emission patterns for different types of biocrusts and bare soil are shown in *SI Appendix*, Table S1. Characteristic emission patterns of NO and HONO at varying soil water contents are shown in Fig. 1; NO_2 emissions were negligible (mostly <5 ng·m^{-2}·s^{-1}). To evaluate whether NO and HONO emissions are initiated biotically or not, dark cyanobacteria-dominated biocrusts were measured as described above, then autoclaved, and after cooling, NO and HONO fluxes were analyzed again (Fig. 3).

Nutrient, Chlorophyll, and pH Analyses. Nitrate, nitrite, and ammonium contents of the soil were determined according to DIN ISO/TS 14256-1 by Envilytix (41). Chlorophyll contents were determined by extracting the biocrust samples twice with DMSO at 60 °C for 90 min each according to the method described by Ronen and Galun (42). Nitrate, nitrite, ammonium content, and biomass of photosynthetically active organisms determined as chlorophyll a and a+b of the samples are shown in the *SI Appendix*, Fig. S3 and Table S6. pH values of each type of biocrust and bare soil (n = 4; *SI Appendix*, Table S7) were determined electrometrically as described by Steubing and Fangmeier (43).

Comparison of Laboratory and Field Conditions During Wetting and Drying Cycle. Laboratory conditions were compared with those occurring in the field to check whether wetting–drying cycles happen in a comparable way. Activity patterns in the field were assessed at 10-min increments using three microclimate stations, which had been installed within the study region for

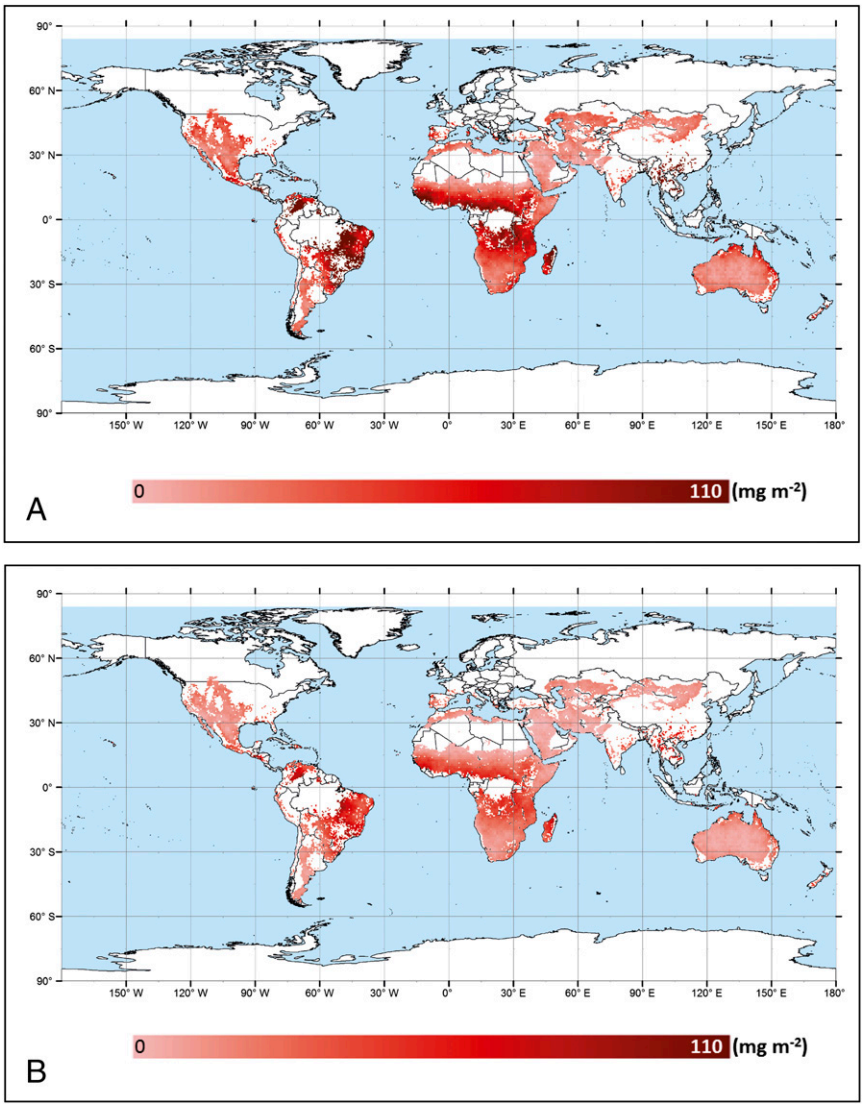

Fig. 4. Annual emissions from biocrusts in desert and steppe ecosystems on a global scale. (*A*) NO-N emissions. (*B*) HONO-N emissions. The flux units are milligrams per square meter per year.

1 y (*SI Appendix*, Table S4). It turned out that the duration of activity after precipitation events in the field was about two times as long as the duration of emissions in the laboratory, thus equaling the ~8 K lower field temperatures, as 10 K lower temperatures are expected to approximately halve the emissions.

Quantification of Habitat Emission per Precipitation Event. NO and HONO emission data integrated over a full wetting and drying cycle were calculated for the different types of biocrusts and bare soil (*SI Appendix*, Table S2). The average composition of biocrusts in dryland areas was assessed compiling field measurements and available literature data (*SI Appendix*,

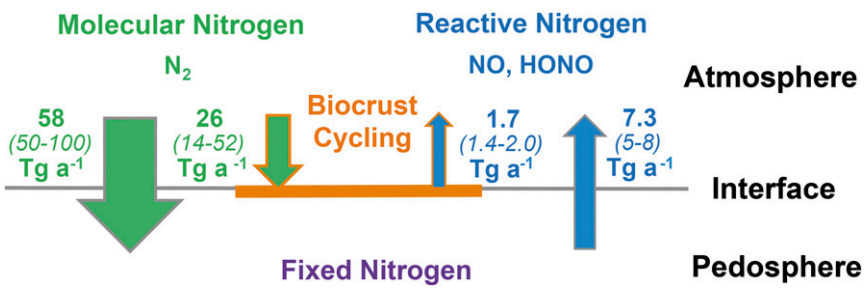

Fig. 5. Relevance of biocrust N fluxes discussed in this paper as part of the global terrestrial biological nitrogen fluxes. Inner arrows represent the global annual fixation of molecular nitrogen by biocrusts, as estimated in a previous study (18), and emission of reactive nitrogen (NO-N plus HONO-N) by biocrusts on the ground surface of drylands, as obtained in this study. Outer arrows indicate the global annual biological fixation of molecular nitrogen and emission of reactive nitrogen (NO_x) by soil under natural vegetation covers as reported in the latest report of the IPCC (19).

Table S3). The field data were collected at the four climate station sites in the Succulent Karoo using the point intercept method as described in ref. 16 at 200 randomly chosen locations per site. The community emissions ($E_{commun,NO}$; $E_{commun,HONO}$) per wetting and drying cycle event (in milligrams of N per square meter) were calculated according to the following:

$$E_{commun} = \sum (E_{N,int,LB} * C_{LB}) + (E_{N,int,DB} * C_{DB}) + (E_{N,int,CB} * C_{CB}) + (E_{N,int,MB} * C_{MB}), \quad [1]$$

where $E_{N,int,type}$ is the biocrust emission per wetting and drying cycle (in milligrams of N per square meter) and C_{type} is the relative cover of biocrust types (in square meters per square meter). Cover types comprise light cyanobacteria-dominated (LB), dark cyanobacteria-dominated (DB), chlorolichen-dominated (CB), and moss-dominated biocrusts (MB).

For calculation of bare soil emissions, when there are no biocrusts present (BS), soil coverage was set to two-thirds and nonemitting surface cover to one-third of total surface cover, as some areas are sealed by buildings and rocks where no emissions are expected. Soil emissions ($E_{soil,NO}$; $E_{soil,HONO}$) per wetting and drying cycle event (in milligrams of N per square meter) were calculated according to the following:

$$E_{soil} = E_{N,int,BS} * 0.6666. \quad [2]$$

Upscaling of Emissions to a Global Scale. As biocrusts mainly occur in arid regions, upscaling was performed for the fractional steppe and desert ecosystems coverage as determined by Elbert et al. (18).

Global emissions of NO and HONO ($E_{glob,NO}$; $E_{glob,HONO}$; in teragrams per year) were calculated according to the following:

$$E_{glob,NO} = \sum_{i=1}^{n} E_{commun,cell,NO} * P_{cell} \quad [3]$$

and

$$E_{glob,HONO} = \sum_{i=1}^{n} E_{commun,cell,HONO} * P_{cell} \quad [4]$$

where i is the grid cell, $E_{commun,cell,NO}$ and $E_{commun,cell,HONO}$ are the community emissions of NO and HONO, respectively, in a grid cell during one precipitation event (in teragrams per year), and P_{cell} is the number of precipitation events of each grid cell.

The annual average number of precipitation events was calculated from 3-hourly spatially downscaled (0.5°) precipitation data for the decade 1999–2008 (44). Each time step with precipitation >0 was counted as one event for each grid cell. For the study region in the Succulent Karoo, the number of precipitation events determined by local climate measurements between October 2008 and 2009 was more than two times higher than the remote sensing data used by us (34 versus 12.3 events per year), again underlining our conservative approach.

Statistics. As uncertainty estimate, generally the SE of means is given. Correlations between NO and HONO emission patterns, maximum NO/HONO fluxes at optimum water content and soil pH, nutrient, and biomass data were analyzed using the Spearman rank test, as no normal distribution of data were achieved. Different soil cover types (i.e., biocrust types and bare soil) were analyzed for differences in maximum NO and HONO fluxes, as well as soil nutrient and biomass data, using a Kruskal–Wallis ANOVA. All statistical tests were performed using Origin Pro-9.

ACKNOWLEDGMENTS. Special thanks go to Burkhard Büdel for supervision of the master thesis of A.T. We thank the editor and two unknown reviewers for stimulating comments. This study was supported by the Max Planck Society (Nobel Laureate Fellowship to B.W.) and the German Research Foundation (Projects WE2393/2-1 and WE2393/2-2 of B.W.). The work of D.W. was supported by the Max Planck Society and Chinese Academy of Sciences. Research in South Africa was conducted with South African Research Permits (22/2008, 38/2009, 86/2013, and 127/2014) and the appending export permits.

1. Monks PS, Granier C, Fuzzi S (2009) Atmospheric composition change–global and regional air quality. *Atmos Environ* 43:5268–5350.
2. Kleffmann J, et al. (2005) Daytime formation of nitrous acid: A major source of OH radicals in a forest. *Geophys Res Lett* 32(5):L05818.
3. Seinfeld JH, Pandis SN (2006) *Atmospheric Chemistry and Physics: From Air Pollution to Climate Change* (Wiley, Hoboken, NJ), 2nd Ed.
4. Galbally IE, Roy CR (1978) Loss of fixed nitrogen from soils by nitric-oxide exhalation. *Nature* 275(5682):734–735.
5. Steinkamp J, Lawrence MG (2011) Improvement and evaluation of simulated global biogenic soil NO emissions in an AC-GCM. *Atmos Chem Phys* 11(12):6063–6082.
6. Pilegaard K (2013) Processes regulating nitric oxide emissions from soils. *Philos T R Soc B* 368(1621):20130126.
7. Su H, et al. (2011) Soil nitrite as a source of atmospheric HONO and OH radicals. *Science* 333(6049):1616–1618.
8. Oswald R, et al. (2013) HONO emissions from soil bacteria as a major source of atmospheric reactive nitrogen. *Science* 341(6151):1233–1235.
9. Hudman RC, et al. (2012) Steps towards a mechanistic model of global soil nitric oxide emissions: Implementation and space based-constraints. *Atmos Chem Phys* 12(16):7779–7795.
10. Dentener FJ (2006) *Global Maps of Atmospheric Nitrogen Deposition, 1860, 1993, and 2050* (Oak Ridge National Laboratory Distributed Active Archive Center, Oak Ridge, TN).
11. Stewart DJ, Taylor CM, Reeves CE, McQuaid JB (2008) Biogenic nitrogen oxide emissions from soils: Impact on NO_x and ozone over west Africa during AMMA (African Monsoon Multidisciplinary Analysis): Observational study. *Atmos Chem Phys* 8(8):2285–2297.
12. Davidson EA, Seitzinger S (2006) The enigma of progress in denitrification research. *Ecol Appl* 16(6):2057–2063.
13. Büdel B, et al. (2009) Southern African biological soil crusts are ubiquitous and highly diverse in drylands, being restricted by rainfall frequency. *Microb Ecol* 57(2):229–247.
14. Noffke N, Christian D, Wacey D, Hazen RM (2013) Microbially induced sedimentary structures recording an ancient ecosystem in the ca. 3.48 billion-year-old Dresser Formation, Pilbara, Western Australia. *Astrobiology* 13(12):1103–1124.
15. Watanabe Y, Martini JEJ, Ohmoto H (2000) Geochemical evidence for terrestrial ecosystems 2.6 billion years ago. *Nature* 408(6812):574–578.
16. Dojani S, Büdel B, Deutschewitz K, Weber B (2011) Rapid succession of biological soil crusts after experimental disturbance in the Succulent Karoo, South Africa. *Appl Soil Ecol* 48(3):263–269.
17. Bowker MA (2007) Biological soil crust rehabilitation in theory and practice: An underexploited opportunity. *Restor Ecol* 15(1):13–23.
18. Elbert W, et al. (2012) Contribution of cryptogamic covers to the global cycles of carbon and nitrogen. *Nat Geosci* 5(7):459–462.
19. Ciais P, et al. (2013) Carbon and other biogeochemical cycles. *Climate Change 2013: The Physical Science Basis. Contribution of Working Group I to the Fifth Assessment Report of the Intergovernmental Panel on Climate Change*, eds Stocker TF, et al. (Cambridge Univ Press, Cambridge, UK).
20. Strauss SL, Day TA, Garcia-Pichel F (2012) Nitrogen cycling in desert biological soil crusts across biogeographic regions in the southwestern United States. *Biogeochemistry* 108(1-3):171–182.
21. Barger NN, Castle SC, Dean GN (2013) Denitrification from nitrogen-fixing biologically crusted soils in a cool desert environment, southeast Utah, USA. *Ecological Processes* 2:16.
22. Abed RMM, Lam P, de Beer D, Stief P (2013) High rates of denitrification and nitrous oxide emission in arid biological soil crusts from the Sultanate of Oman. *ISME J* 7(9):1862–1875.
23. Jaeglé L, Steinberger L, Martin RV, Chance K (2005) Global partitioning of NOx sources using satellite observations: Relative roles of fossil fuel combustion, biomass burning and soil emissions. *Faraday Discuss* 130:407–423, discussion 491–517, 519–524.
24. McCalley CK, Sparks JP (2009) Abiotic gas formation drives nitrogen loss from a desert ecosystem. *Science* 326(5954):837–840.
25. van Dijk SM, et al. (2002) Biogenic NO emissions from forest and pasture soils: Relating laboratory studies to field measurements. *J Geophys Res Atmos* 107(D20):8058.
26. Rummel U, Ammann C, Gut A, Meixner FX, Andreae MO (2002) Eddy covariance measurements of nitric oxide flux within an Amazonian rain forest. *J Geophys Res Atmos* 107(D20):8050.
27. Pratscher J, Dumont MG, Conrad R (2011) Ammonia oxidation coupled to CO_2 fixation by archaea and bacteria in an agricultural soil. *Proc Natl Acad Sci USA* 108(10):4170–4175.
28. Butterbach-Bahl K, Baggs EM, Dannenmann M, Kiese R, Zechmeister-Boltenstern S (2013) Nitrous oxide emissions from soils: How well do we understand the processes and their controls? *Philos T R Soc B* 368(1621):20130122.
29. Barger NN, Belnap J, Ojima DS, Mosier A (2005) NO gas loss from biologically crusted soils in Canyonlands National Park, Utah. *Biogeochemistry* 75(3):373–391.
30. Yienger JJ, Levy H (1995) Empirical model of global soil-biogenic NOx emissions. *J Geophys Res* 100(D6):11447–11464.
31. Bey I, et al. (2001) Global modeling of tropospheric chemistry with assimilated meteorology: Model description and evaluation. *J Geophys Res Atmos* 106(D19):23073–23095.
32. Lenhart K, et al. (2015) Nitrous oxide and methane emissions from cryptogamic covers. *Glob Change Biol* 21(10):3889–3900.
33. Goreau TJ, et al. (1980) Production of NO_2 and N_2O by nitrifying bacteria at reduced concentrations of oxygen. *Appl Environ Microbiol* 40(3):526–532.
34. Stieglmeier M, et al. (2014) Aerobic nitrous oxide production through N-nitrosating hybrid formation in ammonia-oxidizing archaea. *ISME J* 8(5):1135–1146.
35. Wu D, et al. (2014) Novel tracer method to measure isotopic labeled gas-phase nitrous acid ($HO^{15}NO$) in biogeochemical studies. *Environ Sci Technol* 48(14):8021–8027.
36. Brankatschk R, Fischer T, Veste M, Zeyer J (2013) Succession of N cycling processes in biological soil crusts on a Central European inland dune. *FEMS Microbiol Ecol* 83(1):149–160.
37. Reynolds JF, et al. (2007) Global desertification: Building a science for dryland development. *Science* 316(5826):847–851.

38. Hartmann DL, et al. (2013) Observations: Atmosphere and surface. *Climate Change 2013: The Physical Science Basis. Contribution of Working Group I to the Fifth Assessment Report of the Intergovernmental Panel on Climate Change*, eds Stocker TF, et al. (Cambridge Univ Press, Cambridge, UK).
39. Pointing SB, Belnap J (2012) Microbial colonization and controls in dryland systems. *Nat Rev Microbiol* 10(8):551–562.
40. Belnap J, Lange OL (2003) *Biological Soil Crusts: Structure, Function, and Management* (Springer, Heidelberg).
41. Blume HP, et al. (2000) *Handbuch der Bodenuntersuchung* (Wiley-VCH, Weinheim, Germany).
42. Ronen R, Galun M (1984) Pigment extraction from lichens with dimethylsulfoxide (DMSO) and estimation of chlorophyll degradation. *Environ Exp Bot* 24(3): 239–245.
43. Steubing L, Fangmeier A (1992) *Pflanzenökologisches Praktikum* (Ulmer, Stuttgart).
44. Sheffield J, Goteti G, Wood EF (2006) Development of a 50-year high-resolution global dataset of meteorological forcings for land surface modeling. *J Clim* 19(13): 3088–3111.